A time delay compensation strategy for processes with uncertainties

Futao Zhao[1], Yu-Chu Tian[1,2,*], Moses O. Tadé[1] and Hui Li[3]

[1]*School of Engineering, Curtin University of Technology, GPO Box U1987, WA 6845, Australia*

[2]*Computer Engineering Laboratory, School of Electrical and Information Engineering, The University of Sydney, Sydney NSW 2006, Australia*

[3]*Department of Industrial Design and Automation, Beijing Institute of Clothing Technology, Beijing 100020, China*

Abstract

Pattern-based fuzzy predictive (PFP) control, proposed for processes with large time delay, avoids traditional process dynamic models while providing effective disturbance rejection. However, chemical processes often undergo considerable uncertainties, which will affect the performance of the PFP scheme. An extended PFP (EPFP) control scheme is proposed to account for process dynamics with uncertainties. It incorporates a first-order lag unit, viewed as a special filter, with the original PFP, allowing the designer to set a trade-off between performance and robustness. In practice, the filter parameter tuning can be carried out automatically through on-line parameter optimisation. This approach is applied to time delay compensation for a time delayed chemical process with uncertainties. Robustness of the EPFP is analysed via Bode plots under process uncertainties. Illustrative examples are provided to show the effectiveness of the scheme to chemical processes with time delay and uncertainties.

Key words: chemical processes; time delay; predictive control; feature patterns; uncertainties

1. **Introduction**

Time delay, a common feature of many chemical processes because of material and energy transportation, composition analysis, etc., poses a particularly difficult problem for feedback control system. To improve the performance of time-delay systems, special control techniques have been developed, such as the Smith Predictor (SP) (Smith, 1957), the Generalised Analytical Predictor (GAP) (Wellons & Edgar, 1987), and the Internal Model Control (IMC) (Morari & Zafiriou, 1989). All of them provide time delay compensation based on process dynamic models. However, the SP often has poor performance in rejecting load disturbances, which often interfere

*Corresponding author. Tel.: +61-8-9266 3776; fax: +61-8-9266 2681. E-mail: tiany@vesta.curtin.edu.au (Yu-Chu Tian)

with chemical processes (Meyer *et al*., 1976; Astrom & Haggund, 1995; Tian *et al*, 1998a, 1998b). The GAP, an alternative to the SP, provides an improvement in regulatory performance through a disturbance predictor; while it requires an accurate transfer function for load disturbances (Shen & Lee, 1989). The control performance of the SP and GAP will deteriorate, even to the point of instability, if the process/model mismatch occurs (Seborg, *et al*., 1989). The IMC allows the designer to make a trade-off between the closed-loop performance and the robustness in the presence of model mismatch. However, the IMC often provides poor load disturbance suppression when the dynamics of the load disturbance is slower than that of the control channel (Ricker, 1990; Scali, *et al*., 1992; Horn *et al*., 1996). These disadvantages are considerable deterrents to engineering applications of these control techniques. Though great strides have been made to compensate for process time delay, it is still a challenging topic in practice to provide satisfactory control performance for these time-delayed processes.

Chemical processes are often operated under diverse disturbances and uncertainties; it is difficult to develop accurate models for the processes and their disturbances. To alleviate the requirement of accurate mathematical models, some control techniques have been investigated in the past decade, such as the pattern-based control (Cooper *et al*., 1992; Seem, 1998), where adaptive control was developed based on the patterns of process responses instead of the traditional online identification of the process dynamics. Aoki *et al*. (1990) proposed a fuzzy compensation for a glass-melting furnace with time delay. Jang & Chen (1996) constructed a fuzzy model predictive control approach based on the SP structure. A pattern-based fuzzy predictive (PFP) control scheme has been proposed by the authors (Zhao *et al*., 2000). This scheme extracts important information, called feature patterns, from the process time series data of the manipulated and controlled variables and then predicts the controlled variable through fuzzy inference. The advantage of the approach is that it provides the prediction for the effects of both setpoint and load disturbances while avoiding the difficulty of process modelling. In chemical processes, uncertainties are often inevitable during operation. For example, the time delay of a process often varies due to different feed flowrate (Shinskey, 1996). For successful application, the PFP scheme must have the ability to accommodate process uncertainties.

This paper focuses on the performance improvement of the original PFP scheme for chemical processes with uncertainties, particularly the uncertainties of time delay. An extended PFP (EPFP) scheme, incorporating a first-order lag unit with the original PFP, is proposed. The first-order lag unit has two adjustable parameters. This augmented unit not only ameliorates the precision of the original PFP prediction but also improves the stability of the PFP closed-loop

control system in the presence of process uncertainties. The two adjustable parameters can be tuned through on-line parameter optimisation so as to keep an appropriate balance between the control performance and the system robustness. The paper is organised as follows. In Section 2, the original PFP control approach is described. The detrimental effect of variable time delay on the PFP is analysed. The EPFP, an extended pattern-based fuzzy predictive control scheme, is developed in Section 3. Control performance of the EPFP is investigated through simulation examples in Section 4. Finally, conclusions are drawn.

2. Pattern-based fuzzy predictive (PFP) control

Most chemical processes can be described by a first- or second-order plus time delay model. For a process with large time delay, the effects of the control actions (i.e., the fed material or energy) on the process output cannot be displayed immediately. The current feedback signal is not appropriate for the controller to generate pertinent control action for the next step. Therefore, time delay is one of the worst things that can happen to a feedback control loop. To obtain good control performance, it is necessary to predict future values of the process outputs. For illustration, the process output at current time instant k and future time instant $k+d$ can be denoted by convolution integrals

$$C(k) = \sum_{i=d}^{k-d} u(i)g(k-i) + L\sum_{i=k_0}^{k} f(i-k_o) \tag{1}$$

$$C(k+d) = \sum_{i=d}^{k} u(i)g(k+d-i) + L\sum_{i=k_0}^{k+d} f(i-k_o) \tag{2}$$

in which $g(\cdot)$ and $f(\cdot)$ are the impulse response coefficients of the process and the disturbance. L is the disturbance input. k_o is the occurrence time instant of external deterministic disturbance. The difference between $C(k+d)$ and $C(k)$ can be expressed by:

$$\begin{aligned}\Delta C &= C(k+d) - C(k) \\ &= \sum_{i=d}^{k-d} u(i)[g(k+d-i) - g(k-i)] + u(k-d)\sum_{i=k-d}^{k} g(k+d-i) \\ &\quad + \sum_{i=k-d}^{k} [u(i) - u(k-d)]g(k+d-i) + L\sum_{i=k}^{k+d} f(i-k_o)\end{aligned} \tag{3}$$

For convenience, Eq. (3) is expressed as

$$\Delta C = f_1 + f_2 + f_3 + f_4 \tag{4}$$

where f_1, f_2, f_3, and f_4 correspond to the four terms on the right side of Eq. (3), respectively. The physical interpretation of the four items are as follows: f_1 represents the effect of the control inputs before time instant $k - d$; f_2 represents the effect of a step control input $u(k–d)$ during time

period [$k–d$, k]; f_3 represents the effect of the control inputs (deducting $u(k–d)$) during time period [$k–d$, k]; f_4 represents the effect of external disturbance during time period [k, $k+d$]. Clearly, the analytical result of ΔC is difficult to obtain due to the unknown $g(\cdot)$, $f(\cdot)$ and L. It is proposed to develop an alternative method to obtain ΔC.

Chemical processes mostly act as low-pass filters, passing low-frequency signals and attenuating high-frequency signals (Seborg, *et al*., 1989). The process response in the near future may be predicted by extracting the corresponding feature patterns of the present available process behavior by performing necessary cause-and-effect analysis (Bristol, 1977). Most chemical processes have an S-shaped open-loop response, which displays different response trends at different stages. At the first stage (right after the time delay elapses), the response increases with an accelerating rate as a result of the 'energy-storing' effect. After an inflection point, the response remains increasing yet with a decreasing rate, due to the “energy-releasing” effect, until it finally reaches a steady state. This phenomenon reflects the multi-capacity characteristics of a process (Shinskey, 1996). The shape of the response of such a process can always be divided into 'energy-storing', 'energy-releasing', and steady-state phases. Based on the above physical understanding of the process response, the following two feature patterns are extracted from the time series of the measurement of the controlled variable, $\{C(\xi), \xi \le k\}$:

$$S_1 = C(k) - C(k-1) \tag{5}$$

$$S_2 = \sum_{m=1}^{D} \frac{C(k+1-m) + C(k-m-1) - 2C(k-m)}{C(k+1-m) - C(k-m)} \tag{6}$$

where D is the prediction length, S_1 represents an incremental variation of $C(k)$, and S_2 captures the 'energy-storing' and 'energy-releasing' effects on $C(k)$ and indicates the fluctuating trends of S_1. S_1 has the reinforced tendency of increasing if $S_2 > 0$ (the energy-storing phase) and decreasing if $S_2 < 0$ (the energy-releasing phase). S_1 and S_2 reflect the effects of the material or energy fed before the time instant ($k–D$). During the extraction of S_2, $|C(k+1–m) – C(k–m)| > \varepsilon_1$ is inherently assumed, otherwise the corresponding term should be eliminated from S_2. It is obvious that $S_1 = S_2 = 0$ if the process has reached a steady state.

The material or energy fed during the time period [$k–D$, k] does not change the current process output but will affect the process output eventually. The fed material or energy can be imaginarily separated into two parts: $u(k–D)$ and $\{u(k+1-m) - u(k-D), 1 \le m \le D\}$. The former maintains the response trend indicated in S_1 and S_2 while the latter should be characterised using

additional feature patterns. The following two patterns are extracted from the time series of the manipulated variable, i.e., controller output, $\{u(\xi), \xi \le k\}$

$$S_3 = \sum_{m=1}^{D} [u(k+1-m) - u(k-D)] \tag{7}$$

$$S_4 = \left| \frac{1}{DS_3} \cdot \sum_{m=1}^{D} m \cdot [u(k+1-m) - u(k-D)] \right| \tag{8}$$

in which S_3 indicates the accumulation of the control inputs deducting $u(k\text{-}D)$ within the time period $[k–D, k]$, while S_4 assists in determining the effects of S_3. In Eq. (8), it is assumed that $S_3 \neq 0$, otherwise set S_4 to be a large value, such as S_4=1.0.

The extracted feature patterns are used to predict the process output D steps ahead. The prediction algorithm is designed as

$$\hat{C}(k+D) = C(k) + \theta_1 (S_1 + \alpha S_2) + \theta_2 S_3 \tag{9}$$

θ_1, θ_2 and α are three coefficients. With a rough estimate of τ / T_1, Table 1 provides guidelines for determining θ_1 and α. However, the effect of S_3 on the prediction is implicitly affected by S_4 as well as the process characteristic τ / T_1, resulting in the difficulty in expressing θ_2 explicitly. However, θ_2 can be qualitatively described by some rules as summarised in Table 2, where three linguistic values are introduced: Big (B), Medium (M), and Small (S). For τ / T_1, B, M, and S correspond to τ / T_1>2.0, $\in$[0.7, 2.0], and <0.7, respectively; while for S_4, they correspond to S_4> 0.7, $\in$ [0.3, 0.7], and <0.3, respectively.

According to Table 2, τ / T_1 and S_4 are fuzzified. The triangle membership function is used for both τ / T_1 and S_4. From Table 2, nine fuzzy logic rules, which combine qualitative and quantitative information, are designed to infer θ_2. The rules take the form

$$R^j: \ \textbf{If } \tau / T_1 \text{ is } a^j \text{ and } S_4 \text{ is } b^j, \textbf{ Then } \theta_2 \text{ is } c^j \text{ with } \mu^j, \ \ j = 1, \ldots, 9$$

in which a^j, b^j, and c^j are the corresponding linguistic values listed in Table 2 with triangle membership functions $\mu_{aj}(\tau / T_1)$ and $\mu_{bj}(S_4)$. Term μ^j, the membership function of the jth fuzzy rule, is calculated by

$$\mu^j = \min\{\mu_{a^j}(\tau / T_1), \mu_{b^j}(S_4)\} \tag{10}$$

To obtain the actual value of θ_2, a defuzzification procedure is required. Suppose that the central values of the three linguistic values for c^j are c_1, c_2, and c_3, respectively, which can be determined by the least-squares method while constructing the fuzzy rules. θ_2 is computed by the defuzzification relation

$$\theta_2 = \sum_{j=1}^{9} \mu^j c^j / \sum_{j=1}^{9} \mu^j \tag{11}$$

The process output at time instant $k+d$ is predicted by the PFP scheme through Eq. (9) instead of Eq. (3). More information about the fuzzy rule design and pattern-based prediction can be found in (Zhao, *et al.*, 2000). The PFP provides prediction of the process future output without modeling of the process and the disturbances.

3. The EPFP Design

3.1 An extended filter

Chemical processes always contain some uncertainties. The original PFP can withstand considerable process gain uncertainties while its robustness to time delay variation is not satisfactory. To ensure reliable operation of the original PFP in practice, the uncertainty of the process time delay should be taken into account. It can be seen from Eqs. (7) and (8) that the extracted patterns S_3 and S_4 will not exactly describe the real situation of the manipulated variable during the time period $[k–D, k]$ if the process time delay deviates from its nominal value at which the PFP is designed. This situation becomes more severe when the manipulated variable changes significantly during the time period $[k–D, k]$. A graphical illustration of this situation is shown in Figure 1.

In Figure 1, A_i (i=1,2,3,4) is the area enclosed by the corresponding curve and line segment(s). According to different time delay value (d_1 or d_2), the extracted feature pattern S_3 should be

$$S_3 = \begin{cases} A_1, & \mathrm{d} = \mathrm{d}_1 \\ A_1+A_2+A_3, & \mathrm{d} = \bar{d} \\ A_1-A_4, & \mathrm{d} = \mathrm{d}_2 \end{cases} \tag{12}$$

So, if the real time delay of the process d decreases to d_1 or increases to d_2 from $\bar{d}$, even if the variation is small, S_3 will differ remarkably. Accordingly, S_4 will differ as well. If S_3 and S_4 are extracted according to $d = \bar{d}$ as before, the precision of the PFP prediction will be reduced correspondingly, the inaccurate prediction will lead the controller to generate improper manipulated action, which will subsequently worsen the PFP prediction further. In the worst case, the closed-loop control system can be destabilised.

The satisfactory extraction of S_3 and S_4 depends on an accurate estimate of the time delay on-line. But it is very difficult sometimes (Smith & Corripio, 1997). However, the detrimental effect of the time delay variation on S_3 and S_4 will be significantly decreased if the time series, $\{u(\xi), \xi \le k\}$, is smooth (i.e., no fierce fluctuation, no ringing). In this case, A_2, A_3 and A_4 are small. Actually, a smooth manipulated variable time series is practically necessary for

protecting the actuator. To retard performance deterioration of the original PFP and ensure a stable control system under this uncertainty, a first-order lag unit, $F=\theta/(\lambda s+1)$, called 'extended filter' in this paper, is introduced to the PFP to form an EPFP. The filter provides two adjustable parameters for the controlled process under uncertainties while maintaining the original PFP control system design. The function of the filter includes two aspects: 1) to provide improved prediction of the original PFP; and 2) to allow a trade-off between control performance and robustness under process uncertainties.

In chemical process control, disturbance rejection is the major concern; most controllers can be considered regulators. So the EPFP can be moved from the feedback channel to the control channel. The structure of the EPFP is shown in Figure 2, where the time series of the control error is used instead of that of the process output. The EPFP executes prediction based on the process feature patterns and fuzzy logic, which are the combination of qualitative and quantitative description. Ideally, the prediction function of the EPFP (dashed line block of Figure 2) can be described as the following transfer functions,

$$G_{EPFP}=\frac{F}{1+FG_C\overline{G}_P(1-e^{-\overline{\tau}S})} \qquad \text{(for set point disturbance)} \qquad (13)$$

$$G_{EPFP}=[1+\eta\frac{\overline{G}_P(1-e^{-\overline{\tau}S})}{G_Pe^{-\tau S}}]F \qquad \text{(for load disturbance)} \qquad (14)$$

It should be noted that the transcendental transfer functions in Eqs. (13) and (14) are only a conceptual approximation of the EPFP prediction function. In Eq. (14), η = 0 when the control system is at steady state, η = 1 when the control system experiences a load disturbance. We need not determine η additionally because the EPFP realises its prediction function automatically once the effect of a load disturbance is detected by the control system. The closed-loop tracking transfer function of the EPFP is

$$\frac{C}{R}=\frac{FG_CG_Pe^{-\tau S}}{1+FG_C[G_Pe^{-\tau S}+\overline{G}_P(1-e^{-\overline{\tau}S})]} \qquad (15)$$

The regulatory transfer function of the EPFP is

$$\frac{C}{L}=\frac{G_L}{1+FG_C[G_Pe^{-\tau S}+\overline{G}_P(1-e^{-\overline{\tau}S})]} \qquad (16)$$

The characteristic equations of Eqs. (15) and (16) are identical. When the process is operated under its nominal operating point, the time delay term is removed from the characteristic equations and the *F* can be set to unity. However, once the uncertainties of the controlled process emerge, the filter *F* will function effectively to maintain the stability of the closed-loop system. Eqs. (15) and (16) will be used to investigate the robustness of the EPFP in Section 3.3.

3.2 Filter parameters and process uncertainties

To investigate the relationship between the filter parameters and the process uncertainty, a second-order with time delay process is considered:

$$G(s) = \frac{k_p}{(T_1 s + 1)(T_2 s + 1)} e^{-\tau s} \tag{17}$$

The nominal parameters of the process are: $\bar{k}_p = 1.50$, $\bar{T}_1 = 30$, $\bar{T}_2 = 6$, and $\bar{\tau} = 22$. The parameters of the PI controller in the EPFP control system are first tuned with the Ziegler-Nichols tuning method at the nominal operating point. Then, the proportional gain is set to be 30% of the Ziegler-Nichols gain value to ensure the EPFP control system to work under process uncertainties. The settings are $k_c = 1.80$ and $T_I = 20$s. Figure 3 is the filter parameters under process uncertainties, where θ and λ are tuned with respect to the Integral Absolute Error (IAE) of the closed-loop system, the solid line is the filter gain θ and the dashed line is the filter time constant λ. For convenience, the results of the filter parameters θ and λ will be expressed as (θ, λ) hereafter.

Figure 3a indicates the values of θ and λ as the uncertainty of the process steady state gain varies from –50% to 50%. For positive variation of the process gain, θ becomes smaller than 1 and decreases gradually while λ stays at zero.

Figure 3b indicates that θ increases and λ decreases as the uncertainty of the process dominant time constant varies from –30% to 30%. For positive variations of the process dominant time constant, θ becomes greater than 1 and λ stays at zero. For the process inertia uncertainty, λ is equal to zero in most of the cases.

Figure 3c shows the filter parameters under time delay uncertainty. The filter parameters dramatically deviate from (1, 0) under the process time delay uncertainty.

It can be seen from Figure 3 that θ tends to 1 and λ tends to zero as the process uncertainties reduce. If there is no process uncertainty, the extended filter degenerates to unity.

Then the EPFP is identical to the original PFP. θ changes monotonously to the uncertainties of k_p and T_1 and meanwhile λ is a very small number. Therefore, it is recommended to initialise the filter to be (1, 0) *a priori*. To ensure the reliable operation of the EPFP and the stability of the closed control system, a small θ and a large λ are recommended to accommodate the time delay uncertainty, e.g., (0.5, 3.0). It is noted that the relationship shown in Figure 3 is basically applicable to other processes governed by Eq. (17).

The filter provides two adjustable parameters for the EPFP to improve its performance under process uncertainties. A small θ and a big λ can improve the control system robustness, although this will sacrifice the closed-loop control performance. With fixed filter settings, the control performance will be unduly conservative if the process uncertainties reduce significantly. Performance and robustness of a closed-loop control system are usually two contradictory factors. On the other hand, for the EPFP, appropriately increasing θ will be beneficial to tight suppression of load disturbance whose dynamics is slower than that of the process, but appropriately reducing θ will be beneficial to the closed-loop control system stability when the disturbance dynamics is much quicker than that of the process. To ensure a suitable performance, the filter parameters should be detuned in different cases. To keep an appropriate balance between control performance and robustness, a parameter-optimisation scheme is proposed to automatically tune the parameters of (θ, λ) in real time. The optimisation objective index is chosen to be

$$J(\theta, \lambda) = \sum_{k=0}^{N}[(1-r)e^2(k) + r\Delta u^2(k)] \tag{18}$$

in which the first term evaluates the control performance, the second term evaluates the closed-loop robustness, and r a weighting coefficient. This objective function is the same as that of a linear quadratic optimal control. The purpose of penalizing the increment of the manipulated variable in the quadratic objective function is to smoothen the time series $\{u(\xi), \xi \le k\}$. From the aforementioned analysis, it is known that the EPFP is affected by the time delay uncertainty because with deviations from the nominal time delay, the extracted feature pattern S_3 and S_4 cannot reflect the actual situation of the manipulated variable during the time period [k-d, k]. However, the detrimental effect of the time delay variation on S_3 and S_4 will be significantly reduced if the time series $\{u(\xi), \xi \le k\}$ becomes smooth.

The value of r is within [0, 1]. Its effect is not reflected directly in the closed-loop transfer functions of interest. It is difficult to setup an explicit relationship between the value of r and specified robustness characteristics of the EPFP control system. Generally, r is determined by

trial and error. Increasing r in Eq. (18) is similar to increasing an IMC filter coefficient to put emphasis on system robustness (Garcia, *et al*., 1989; Scali, *et al*, 1992). In the extreme case, selecting r=0, the EPFP control system with the optimised filter can be most aggressive and easy to lose its stability. If selecting r = 1, the optimised filter will be (0, *). With this filter parameters, the control signal generated by the EPFP is zero and the whole control system becomes an open loop. In practice, a conservative but reliable tuning is often preferable. Choosing the coefficient as $0.90 \le r \le 0.98$ is recommended. The optimisation of the filter parameters in this study is executed under a step change in setpoint.

3.3 Robustness analysis

Reconsider the process of Eq. (17) with $\bar{k}_p$ = 1.50, $\bar{T}_1$ = 30, $\bar{T}_2$ = 6, and $\bar{\tau}$ = 22. The EPFP is independent of the process model, however, it is designed under a certain operating condition of the process, it will be inevitably subjected to process uncertainties. When the process deviates from the nominal operating conditions, the stability and robust performance of the EPFP should be investigated. As shown in Eqs. (15) and (16), the EPFP's characteristic equations of tracking and regulation are the same, we focus on the Bode plots of the tracking response for time delay uncertainty. The robustness of the EPFP scheme is investigated via Bode plot. For comparison, the Bode plot of the original PFP scheme is also investigated. The filter parameters for the EPFP are (0.51, 6.10) which are obtained through the optimisation with r = 0.98 under the nominal operating conditions. The controllers in the EPFP and the original PFP schemes take the same parameters that k_c = 1.80 and T_I = 20s. Two cases of the process uncertainty are investigated:

Case 1: process time delay increasing to 29 (+30% time delay uncertainty);

Case 2: process time delay decreasing to 15 (–30% time delay uncertainty).

Figure 4a is the closed-loop frequency plot with the process time delay increasing to 29 (Case 1: +30% uncertainty). The peak value of Amplitude Ratio (AR) for the EPFP scheme is 1.16 and for the original PFP is 1.37. When the phase angle of the EPFP is –180º, the frequency of the EPFP closed-loop control system is ω = 0.053 and the corresponding Amplitude Ratio is AR = 0.946. When the phase angle of the original PFP is –180º, the corresponding frequency is ω = 0.067 and Amplitude Ratio is AR = 1.135. The results show that the closed-loop EPFP control system is still stable while that of the original PFP becomes unstable under this situation.

Figure 4b is the closed-loop frequency plot with the process time delay decreasing to 15 (Case 2: –30% uncertainty). The peak value of Amplitude Ratio (AR) for the EPFP scheme is 1.0

and for the original PFP is 1.25. When the phase angle of the EPFP is –180º, the corresponding frequency is ω = 0.065 and Amplitude Ratio is AR = 0.88. When the phase angle of the original PFP is –180º, the corresponding frequency is ω = 0.134 and Amplitude Ratio is AR = 1.082. The results also show that the closed-loop EPFP control system is still stable while that of the original PFP becomes unstable under this process uncertainty. Compared with the original PFP scheme, the EPFP's robustness is improved through the augmented filter.

3.4 On-line realisation of the EPFP

Application of the EPFP scheme involves the following steps. The time series of control error $\{e(\xi), \xi \le k\}$ is used instead of $\{C(\xi), \xi \le k\}$ for the extraction of S_1 and S_2.

Step 1. Initialisation. Determine values for D, α, θ_1, ε_1, ε_2, and the filter parameters (θ, λ). Guidelines in Table 1 can be used to determine α and θ_1.

Step 2. Record the current process output time series of the process output C(k) and the control signal u(k). Calculate the control error e(k).

Step 3. Extract S_1 according to Eq. (5). Set m = 1.

Step 4. If $m>D$, go to Step 5; otherwise, extract S_2 according to Eq. (6). The corresponding accumulation item in Eq. (6) is set to zero if $|e(k+1-m)-e(k-m)| < \varepsilon_1$. Extract S_3 and S_4 according to Eqs. (7) and (8), respectively. If $|S_3| < \varepsilon_2$, set S_4 = 1.0. Increase m by 1, and go back to Step 4.

Step 5. Fuzzification of τ / T_1 and S_4.

Step 6. Calculate the membership functions of $\mu_{a^j}(\tau / T_1)$ and $\mu_{b^j}(S_4)$.

Step 7. Calculate μ^j according to Eq. (10). Increase j by 1. If j > 9, go to Step 8; else go back to Step 7.

Step 8. Calculate θ_2 according to Eq. (11).

Step 9. Calculate the prediction $\hat{e}(k+D)$ according to Eq. (11) in which the control error is used instead of the process output. Feed the prediction $\hat{e}(k+D)$ to the controller through the filter F. Go to Step 2 for the computation of the next sampling period.

4. Performance investigation

Reconsider the process of Eq. (17) with nominal parameters as: $\bar{k}_p$ = 1.50, $\bar{T}_1$ = 30, $\bar{T}_2$ = 6, and $\bar{\tau}$ = 22. The performance investigation of the EPFP focuses on the process time delay and its uncertainties. Time unit is second. Sampling period is T_S = 1s and the simulation period is N =

1000s. A step change in setpoint from 0 to 1.0 occurs at k = 0, which is followed by a unit step change of the following disturbance at k=500s.

$$G_L(s) = 1.5/(50s+1)$$

For comparison, the schemes of the EPFP, the SP (Smith predictor), and a direct PI control (that does not incorporate any prediction scheme) are studied. All three schemes use a PI controller whose transfer function is $G_C = k_c(1+1/T_I s)$. The parameters of the PI controller for the three control schemes are all tuned at the nominal operating point with Ziegler-Nichols controller setting at first. The proportional gain of the PI controller in both EPFP and SP schemes is set to be 30% of the corresponding Ziegler-Nichols tuning result. The final settings are tabulated in Table 3. The parameter values for the realisation of the EPFP are chosen as: D = 24, α = 0.21, θ_1 = 0.7D, θ = 0.51, λ = 6.1, and $\varepsilon_1 = \varepsilon_2$ = 0.001. The central values of three linguistic terms B, M, and S for θ_2 have been identified as 0.02, 0.0185, and 0.017, respectively. The simulation is carried out on a MATLAB®/ SIMULINK™ platform.

4.1 EPFP with a fixed filter

To accommodate large uncertainties of the process, the filter parameters (θ, λ) are optimised under the nominal time delay with the weighting coefficient r = 0.98. The optimisation result is (0.51, 6.10). The performance indices (IAE) of the three schemes are compared.

The control performance of the EPFP under the nominal time delay value is investigated first. Figure 5 shows that the SP provides the best performance among the three schemes in this case. The EPFP's performance is also satisfactory, better than that of the direct PI controller.

If the filter in the EPFP is set as (1, 0), the EPFP is identical to the original PFP. Its performance index is IAE = 64.23. Though the filter (0.51, 6.10) in EPFP makes the EPFP's performance inferior to that of the SP scheme, it improves the robustness of the EPFP scheme. To investigate the robustness of the EPFP, the control performances of the EPFP with the fixed filter (0.68, 3.49) under ±30% time delay uncertainties are shown in Figures 6 and 7.

Figure 6 shows the performances of the three control schemes when the process time delay increases by 30% to 29. It is noticeable that the stability of the SP scheme is the worst. The SP's response is seriously oscillatory in this case. Meanwhile the EPFP and the direct PI schemes are stable. The performance index of the EPFP is the best.

In Figure 7, the process time delay decreases by 30% to 15. In this case, the EPFP scheme still works well, while the SP scheme becomes unstable (and thus the SP response is not drawn). The performance index of the EPFP scheme is also better than that of the direct PI control.

4.2 EPFP with optimised filter

To accommodate various process uncertainties, the filter parameters are often conservatively set *a prior*. If the filter parameters are optimised on-line, the EPFP can adapt to different process uncertainties with an appropriate balance between control performance and robustness. The EPFP's performances under ±30% time delay uncertainties are investigated with the on-line adaptation of the filter parameters. The weighting coefficient is selected as $r = 0.90$.

When the process time delay increases by 30% to 29, the optimised filter parameters are (0.45, 2.98). With this filter parameter setting, the performance index of the EPFP is IAE = 111.7 which is better than that with a fixed filter (0.51, 6.10) as shown in Figure 6, where the corresponding performance index is IAE = 118.3.

When the process time delay decreases by 30% to 15, the optimised filter parameters are (0.80, 10.0). With this filter parameter setting, the performance index of the EPFP is IAE = 71.7 which is better than that with a fixed filter (0.51, 6.10) as shown in Figure 7, where the corresponding performance index is IAE = 93.1.

With on-line optimisation of the filter parameters, the EPFP' s performance is improved and its applicable range is extended for large process uncertainties. To further verify the effectiveness of the EPFP design, the combined uncertainties of τ, k_p, and T_1, are investigated under the following nine cases:

Case 1: $\tau = 29,\ k_p = 2.25,\ T_1 = 39$

Case 2: $\tau = 29,\ k_p = 2.25,\ T_1 = 21$

Case 3: $\tau = 29,\ k_p = 0.75,\ T_1 = 39$

Case 4: $\tau = 29,\ k_p = 0.75,\ T_1 = 21$

Case 5: $\tau = 15,\ k_p = 2.25,\ T_1 = 39$

Case 6: $\tau = 15,\ k_p = 2.25,\ T_1 = 21$

Case 7: $\tau = 15,\ k_p = 0.75,\ T_1 = 39$

Case 8: $\tau = 15,\ k_p = 0.75,\ T_1 = 21$

Case 9: $\tau = \bar{\tau},\ k_p = \bar{k}_p,\ T_1 = 15,\ T_2 = 9$

For briefness, the response figures of the above nine cases are left out here, their corresponding IAEs are tabulated in Table 4. The corresponding optimised parameters of the filter are also provided in the table. The performance of the EPFP scheme is evidently superior to that of the SP and direct PI schemes under these process uncertainties. Meanwhile, the SP scheme becomes unstable in Cases 2, 5 and 6 and the direct PI control becomes unstable in Case 2. The results in Table 4 demonstrate the effectiveness of the EPFP scheme to control a chemical process with time delay and uncertainties. Case 9 is a special situation where the two time constants of the second-order process become close (T_1 decreases by 50% to 15 s while T_2 increases by 50% to 9 s). In this case, the EPFP still demonstrates its superior performance to that of the SP and direct PI control schemes.

5. Conclusions

An extended pattern-based fuzzy predictive (EPFP) control strategy, augmented with an "extended filter" to accommodate the uncertainties of chemical processes with large time delay, is developed in this paper. By using on-line optimisation of the filter, the EPFP keeps an appropriate balance between performance and robustness. The undesirable effects of process time delay, particularly its uncertainty, on a feedback control system is effectively reduced. Simulation results have demonstrated the effectiveness and feasibility of the EPFP on time delay compensation. Issues that are not addressed in this paper but deserved further investigation include integration of the filter and controller in the EPFP scheme and provision of tuning guideline for this integrated unit.

Nomenclature

Symbols

a,b,c	linguistic values for fuzzy sets
AR	amplitude ratio
C	controlled variable
ΔC	$C(k+d) - C(k)$
d	time delay, $d = \tau/T_S$
d_1, d_2	process real time delay at a certain moment
D	prediction length, $D \geq d$
e	control error, $e = R - C$
e_c	signal fed to controller
$f(\cdot)$	impulse response coefficients of disturbance
F	extended filter
$g(\cdot)$	impulse response coefficients of the controlled process
G	the actual process with time delay term
Gc	controller
G_L	the disturbance process
G_P	the actual process without time delay term
k	present sampling instant
k_c	controller proportional gain
k_o	the occurrence time instant of disturbance
k_p	process steady-state gain
L	disturbance input
N	simulation time period
R	set point
r	weight coefficient (≥ 0)
s	complex variable used in Laplace transform
S_i	feature patterns (i = 1, 2, 3, 4)
T_1	process dominant time constant
T_2	process time constant
T_I	controller integral time
T_S	sampling period
u	manipulated variable
$\Delta u(k)$	variation of manipulated variable, i.e., $\Delta u(k) = u(\mathrm{k}) - u(\mathrm{k\text{-}1})$
z^{-1}	backward shift operator

Greek letters

α	coefficient
ε_1, ε_2	thresholds
η	on-off coefficient (η = 1 or 0)
θ	filter gain
θ_1, θ_2	coefficients
λ	filter time constant
μ	membership function
τ	time delay, $\tau = d\ T_S$
ω	frequency

Hat over variables

-	nominal value
^	prediction

References

Aoki, S., Kawachi, S. and Sugeno, M. (1990). Application of fuzzy control logic for dead time processes in a glass melting furnace, *Fuzzy Sets and Systems*, 38(3), 251-265.

Astrom, K.J. and Hagglund, T. (1995). PID controllers: Theory, design and tuning, 2nd Edition, Research Triangle Park, NC.

Bristol, E.H. (1977). Pattern recognition: an alternative to parameter identification in adaptive control, *Automatica*, 13(2), 197-202.

Cooper, D.J., Megan, L. and Hind Jr, R.F. (1992). Comparison two neural networks for pattern-based adaptive process control, *AIChE J.*, 38(1), 41-45.

Garcia, C.E., Prett, D.M. and Morari, M. (1989). Model predictive control: theory and practice - a survey, *Automatica*, 25(3), 335-348.

Horn, I.G., Arulandu, J.R., Gombas, C.J., Vanantwerp, J.G and Braatz, R.G. (1996). Improved filter design in internal model control, *Ind. Eng. Chem. Res.*, 35(10), 3437-3441.

Jang, M.J. and Chen, C.L. (1996). Fuzzy successive modelling and control for time-delay system, *Int. J. System Sci.*, 27(12), 1483-1490.

Meyer, C., Seborg, D.E. and Wood, R.K. (1976). A comparison of the Smith Predictor and conventional feedback control, *Chem. Eng. Sci*., 31(9), 775-778.

Morari, M. and Zafiriou, E. (1989). Robust process control, Prentice-Hall. Englewood Cliffs, NJ.

Ricker, N.L. (1990). Model predictive control with state estimation, *Ind. Eng. Chem. Res*., 29(3), 374-382.

Scali, C., Semino, D. and Morari, M. (1992). Comparison of internal model control and linear quadratic optimal control for SISO systems, *Ind. Eng. Chem. Res.*, 31(8), 1920-1927.

Seborg, D.E., Edgar, T.F. and Mellichamp, D.A. (1989). Process dynamics and control, John Wiley, NY.

Seem, J.E. (1998). A new pattern recognition adaptive controller with application to HVAC systems, *Automatica*, 34(8), 969-982.

Shen, G.C. and Lee, W.K. (1988). Generalized Analytical Predictor, *AIChE J.*, 34(4), 676-678.

Shinskey, F.G. (1996). Process control system, 4th Edition, McGraw-Hill, NY.

Smith, C.A. and Corripio, A.B. (1997). Principles and practice of automatic process control, 2nd Edition, John Wiley & Sons, NY.

Smith, O.J. (1957). Closer control of loops with dead time, *Chem. Eng. Process*, 53(5), 217-219.

Tian, Y.C. and Gao, F. (1998a). A double-controller scheme for control of processes with dominant delay, *IEE Proc. Control Theory & Appl.*, 145(5), 479-484.

Tian, Y.C. and Gao, F. (1998b). Compensation of dominant and variable delay in process systems. *Ind. Eng. Chem. Res.*, 37(3), 982-986.

Wellons, M.C. and Edgar, T.F. (1987). The generalized analytical predictor, *Ind. Eng. Chem. Res*., 26(8), 1523-1536.

Zhao, F., Ou, J. and Du, W. (2000). Pattern-based fuzzy predictive control for a chemical process with dead time, *Eng. Appl. Artificial Intelligence*, 13(1), 37-45.

Captions of illustrations

Table 1
Recommendation for selection of θ_1 and α

τ / T_1	0.1	0.2	0.6	1.0	2.0	3.0	5.0
θ_1	$0.9D$	$0.8\,D$	$0.7\,D$	$0.6\,D$	$0.5\,D$	$0.4\,D$	$0.3\,D$
α	0.25	0.23	0.21	0.18	0.14	0.12	0.08

Table 2
The qualitative effect of τ / T_1 and S_4 on θ_2

τ / T_1	B	B	B	M	M	M	S	S	S
S_4	B	M	S	B	M	S	B	M	S
θ_2	S	M	B	S	M	M	S	S	M

Table 3
Controller parameter settings

Settings	EPFP	SP	Direct PI
k_c	1.80	2.80	0.75
T_I (s)	20.0	11.6	72.0

Table 4

Performance indices of the EPFP (with optimisation of the filter), SP, and direct PI control schemes under the process different uncertainties

Process uncertainties		Case 1	Case 2	Case 3	Case 4	Case 5	Case 6	Case 7	Case 8	Case 9
Filter (θ, λ) for EPFP	θ	0.33	0.25	0.95	0.92	0.58	0.56	2.04	1.99	0.47
	λ	1.89	1.84	7.25	7.52	6.05	29.02	22.16	28.24	2.47
IAE	EPFP	108.20	118.38	132.47	117.26	66.14	81.47	88.96	75.03	100.00
	SP	171.41	+	156.48	149.96	+	+	153.83	208.41	118.68
	PI	253.50	+	238.54	236.11	93.02	113.11	237.21	234.13	145.63

+ : Denotes closed-loop unstable.

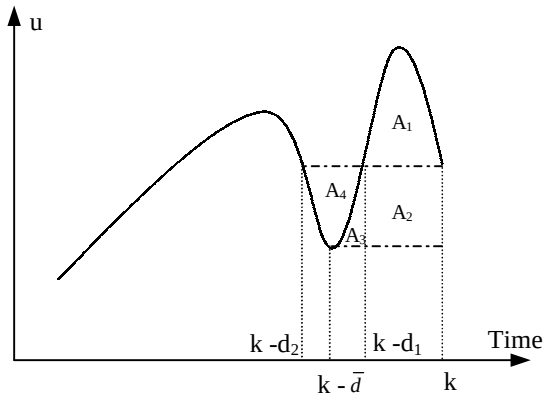

Figure 1. The effect of time delay variation on feature pattern S_3.

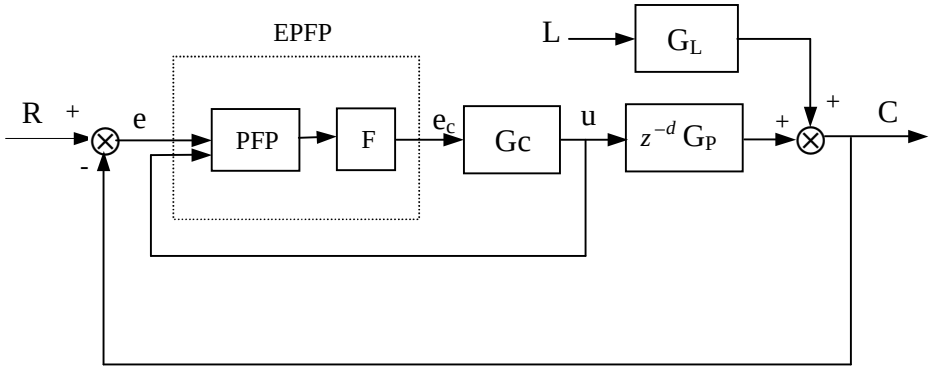

Figure 2. Diagrammatic structure of the EPFP control structure.

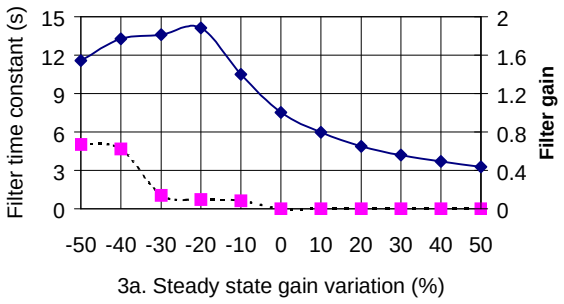

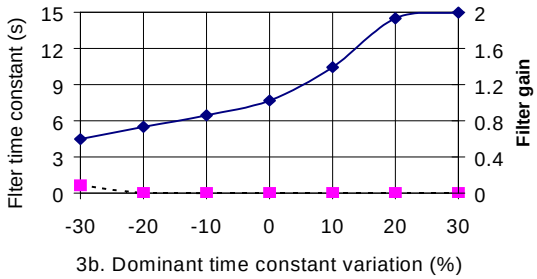

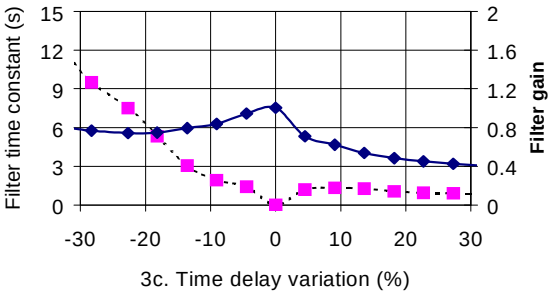

Figure 3. Relationship between the filter parameters and the process uncertainties.

(—◆— : filter gain; ···■··· : filter time constant)

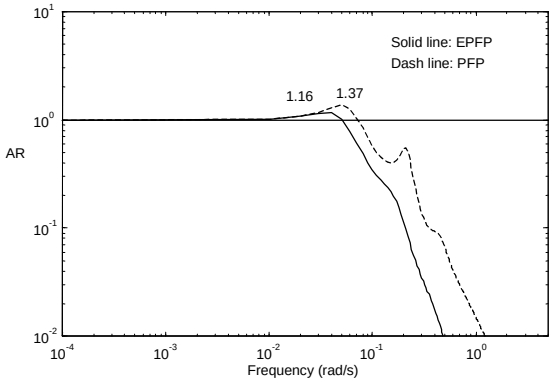

4a. Case 1: +30% time delay uncertainty.

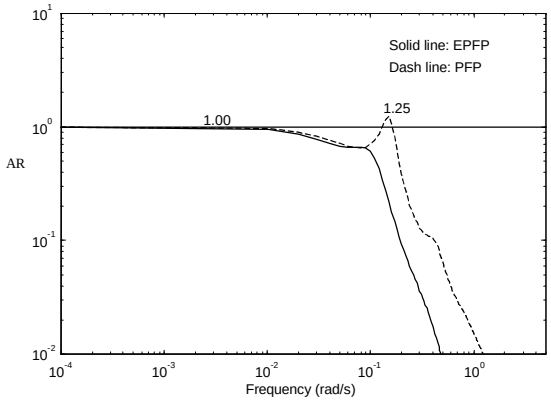

4b. Case 2: -30% time delay uncertain.

Figure 4. Closed-loop Bode plots of the EPFP control system under time delay uncertainties

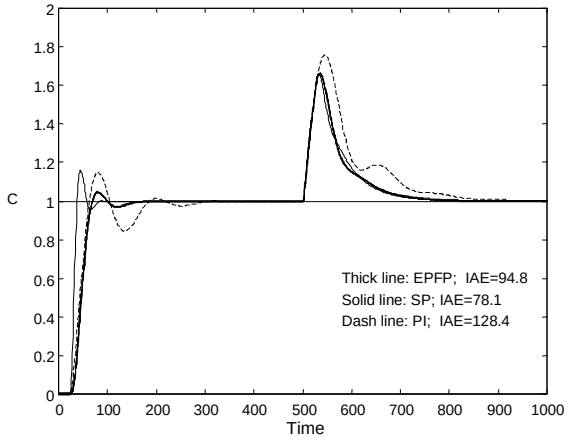

Figure 5. Performance under nominal time delay (τ=22) with a fixed filter (0.51, 6.10).

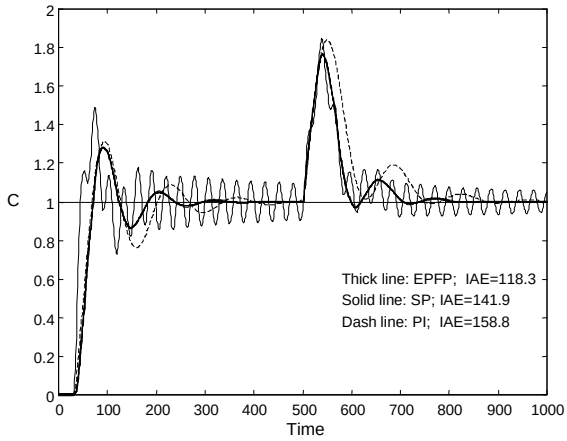

Figure 6. Performance under +30% time delay variation (τ=29) with a fixed filter (0.51, 6.10).

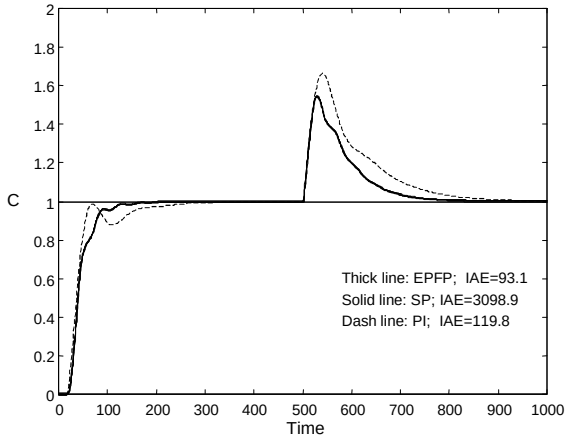

Figure 7. Performance under +30% time delay variation (τ=29) with a fixed filter (0.51, 6.10).